Novel Topotactic Conversion of an Organically Templated Vanadyl Phosphate Framework into Layered Structures

Minakshi Asnani,[a] Sanjeev Sharma,[a] Samuel E. Lofland,[b] Kandalam V. Ramanujachary,[b] Philippe A. Buffat,[c] and Arunachalam Ramanan*[a]

Keywords: Vanadyl phosphate / Topotactic / Intercalation / Ion exchange

This paper reports a novel topotactic exchange reaction of the ethylenediammonium intercalated mixed-valent vanadyl phosphate, $(H_3NCH_2CH_2NH_3)_{0.5}[V^{4+}{}_{0.45}V^{5+}{}_{0.55}O_2PO_4\{P(OH)_2\}_{0.483}]$, with monovalent cations at room temperature. Alkali metal ions and other monovalent cations (e.g. K^+, Rb^+, Tl^+, NH_4^+) behave similarly, leading to intercalated layered vanadyl phosphates (basal spacing about 6.3–6.5Å). The amount of cations incorporated between the layers is essentially dictated by the charge present on the layers (equivalent to the amount of V^{4+} present). The present approach has enabled us to obtain a new phase, $Tl_{0.45}VOPO_4{\cdot}0.33H_2O$, under ambient conditions. All the layered solids show low-temperature magnetic behaviour similar to hydrothermally synthesised products. Treatment with silver ions resulted in a new silver vanadium(V) phosphate $Ag_{3.5}VP_{1.5}O_8$ [monoclinic; $a = 22.557(4)$, $b = 7.973(3)$, $c = 12.430(3)$ Å and $\beta = 112.26(2)°$] coated with silver metal nanospheres (ca. 15 nm) which, on heating above 400 °C, yielded a 2:1 mixture of two thermodynamically stable phases, $Ag_2VO_2PO_4$ and Ag_3PO_4.

Introduction

Inorganic layered materials have received considerable attention as hosts for the intercalation of guest molecules and ion exchange reactions.[1] Intercalation compounds of vanadyl phosphate with aliphatic and aromatic amines,[2] heterocycles,[3] alcohols and diols[4] as well as carboxylic acids[5] and their amides[6] have been extensively studied. Vanadyl phosphates are important materials owing to their potential uses as sensors, fuel cells and catalysts for the oxidation of hydrocarbons.[7,8] Intercalated vanadyl phosphates can be synthesised either through direct hydrothermal treatment or via ion-exchange reactions.[9−16] The ion-exchange behaviour of several organically intercalated oxides is well-known.[17,18] However, to the best of our knowledge, exchange reactions with organically intercalated vanadyl phosphates have not been reported. In this paper, we describe a novel room temperature topotactic reaction of ethylenediammonium intercalated vanadyl phosphate with various metal ions. Our investigations reveal that only monovalent ions viz. K^+, Rb^+, Tl^+ and NH_4^+ undergo facile exchange reactions with ethylenediammonium intercalated vanadyl phosphate. The reaction with silver ions is unusual since it leads to the formation of a hitherto unknown silver vanadium phosphate coated with silver nanoparticles.

Results and Discussion

A single-crystal structure analysis of the parent compound, ethylenediammonium intercalated mixed-valent vanadyl phosphate, $(H_3NCH_2CH_2NH_3)_{0.5}[V^{4+}{}_{0.45}V^{5+}{}_{0.55}O_2PO_4\{P(OH)_2\}_{0.483}]$ (hereafter referred to as enVPO) has been reported earlier.[19] The crystal structure of this phase is analogous to that of $(H_3NCH_2CH_2NH_3)$ $[(VO)_2(PO_4)_2(H_2PO_4)]$ reported by Harrison et al.[20] except that the phosphate groups linking the vanadyl phosphate layers (VPO) are partially disordered in our case. The structure contains layers consisting of VO_5 square pyramids and PO_4 tetrahedra sharing vertices in the *ab*-plane. VO_5 groups in adjacent layers are connected through a disordered tetrahedral $PO_2(OH)_2$ unit and the unprotonated oxygen atoms of these tetrahedra can also be considered as a part of the vanadium octahedra with long V−O bonds (2.2 Å) (Figure 1). The VPO configuration results in puckered $[VO_2PO_4]^{2-}$ layers oriented in the [101] direction. The layers are connected by $PO_2(OH)_2$ tetrahedral units to form a 3D network along the *c*-axis. Ethylenediammonium cations occupy the cavities formed between the $PO_2(OH)_2$ tetrahedra in the interlayer region. The open framework structure of

---

[a] Department of Chemistry, Indian Institute of Technology,
New Delhi 110016, India
Fax: (internat.) + 91-11-26582037
E-mail: aramanan@chemistry.iitd.ac.in
[b] Department of Chemistry and Biochemistry, Rowan University,
Glassboro, NJ 08028, USA
[c] EPFL,
1015 Lausanne, Switzerland

enVPO makes the organic cation and the bridging phosphate group accessible to metal cation guest species. In this work, we attempted to exchange the ethylenediammonium cation with various metal ions. Before every exchange reaction, care was taken to ascertain the single-phase nature of enVPO using powder X-ray diffraction, TGA, DTA, cerimetric titration and EDAX. Initial reactions indicated that enVPO was quite stable in aqueous solutions for several days in the presence of lithium, sodium, cesium and various divalent metal ions (Mg^{2+}, Ca^{2+}, Mn^{2+}, Co^{2+}, Ni^{2+} or Cu^{2+}). A reaction occurred only when the metal ion was potassium, rubidium, thallium, ammonium or silver. A preliminary analysis clearly showed the presence of both ethylenediammonium and phosphate groups in the filtrate.

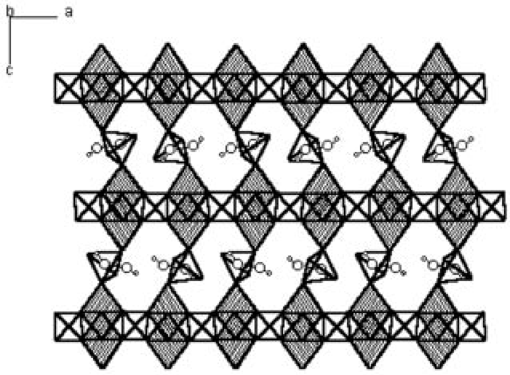

Figure 1. Crystal structure of enVPO viewed along *b* axis; during the exchange reaction, the bridging phosphate groups (coloured orange) and the ethylenediammonium cations leach out

Reactivity with Metal Ions and the Ammonium Ion

EnVPO undergoes a facile exchange reaction with K^+, Rb^+, Tl^+ and NH_4^+ under mild conditions to form metal or ammonium intercalated vanadyl phosphates, M_xVPO (M = K, Rb, Tl and NH_4). Powder X-ray diffraction patterns of the exchanged products were very different from that of parent enVPO (Figure 2) with a basal spacing of 7.9Å. The presence of dominant 00l reflections in the products indicates strong lamellar characteristics ($c \approx$ 6.3−6.5Å) similar to other metal intercalated layered vanadyl phosphates. In the cases of the potassium,[21−24] rubidium[21−26] and ammonium[26,27] incorporated solids, the observed basal spacings were similar to those reported in the literature. Furthermore, powder X-ray diffraction patterns of the exchanged products matched well with simulated patterns of metal intercalated vanadyl phosphates.[11,12] While the parent enVPO did not contain any water molecules, the exchanged products M_xVPO were hydrated as indicated by FTIR spectroscopy and thermal analyses. The amount of water and the phase changes of the solids were determined by TGA and DTA studies (Figure 3). Upon heating, all solids exhibited an initial weight loss below 100 °C. K_xVPO showed an additional weight loss of 6.3% in the temperature range 150 to 230 °C. Above this temperature there were no further weight losses. Rb_xVPO also showed similar thermal behaviour. $(NH_4)_x$VPO exhibited two additional weight losses, namely 6.6% in the temperature range 130 to 200 °C and a broad weight loss of 8.3% in the temperature range 210 to 430 °C. Thallium intercalated vanadyl phosphate Tl_xVPO, exhibited a much lower weight loss (<2%) suggesting very little incorporation of water. It should be mentioned here that thallium intercalated vanadyl phosphate, Tl_xVPO has been synthesised for the first time by a low temperature method in this study. DTA of all the solids showed a broad endothermic peak corresponding to the loss of water molecules except in $(NH_4)_x$VPO in which it also includes loss of ammonia. In all cases, the products were X-ray amorphous after heating above 300 °C.

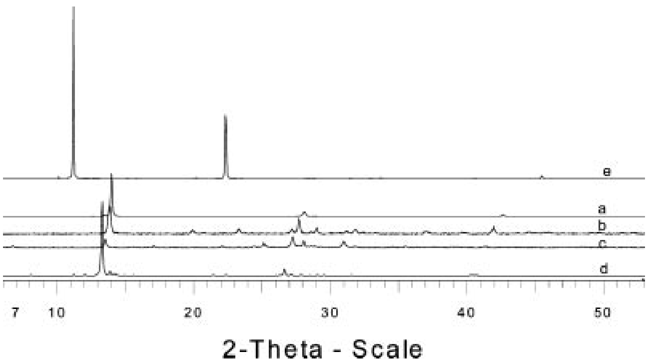

Figure 2. Powder X-ray patterns of (a) K_xVPO, (b) Rb_xVPO, (c) Tl_xVPO, (d) $(NH_4)_x$VPO and (e) enVPO

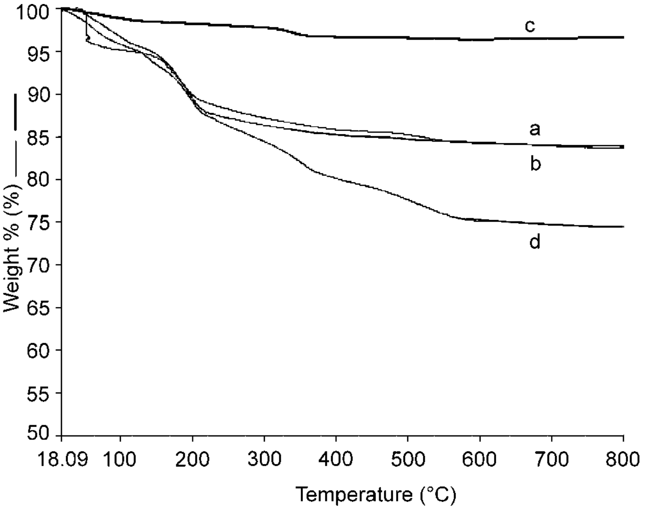

Figure 3. TGA curves of (a) K_xVPO, (b) Rb_xVPO, (c) Tl_xVPO and (d) $(NH_4)_x$VPO

The absence of the ethylenediammonium ion was further confirmed by FTIR spectroscopy. All the exchanged solids showed the presence of strong bands around 1055 and 940 cm^{-1} due to PO_4 groups, a peak around 990 cm^{-1} due to the V=O stretch and, similar to alkali metal intercalated vanadyl phosphates, a broad weak band around 680 cm^{-1} due to the V−O−P lattice.[10,11] In the case of $(NH_4)_x$VPO, additional peaks were observed around 3300 and 1350 cm^{-1} due to N−H stretching and bending vibrations. SEM

$$\begin{aligned}&(H_3NCH_2CH_2NH_3)_{0.5}[V^{4+}{}_{0.45}V^{5+}{}_{0.55}O_2PO_4\{P(OH)_2\}_{0.483}] + 0.45M^{+}(aq) + yH_2O \longrightarrow \\ &M^{+}{}_{0.45}V^{4+}{}_{0.45}V^{5+}{}_{0.55}OPO_4.yH_2O + 0.5[H_3NCH_2CH_2NH_3]^{2+}(aq) + 0.966[H_2PO_4]^{-}(aq) + 0.034(OH)^{-}(aq)\end{aligned} \tag{1}$$

studies revealed a plate like morphology for all solids which is similar to metal intercalated layered vanadyl phosphates.[11] Cerimetric titrations showed that the V^{4+}/V^{5+} ratio in the parent enVPO as well as in the metal exchanged products remained almost the same within experimental error. EDAX analysis indicated that the P/V ratio in the parent enVPO was about 1.5 which is closer to the composition established by a single-crystal X-ray diffraction analysis.[19] However, in the exchanged products, the P/V ratio was about 1 with $x \approx 0.5$ for all solids. On the basis of powder X-ray diffraction, TG, EDAX and chemical analyses, we established the general composition $M_xVOPO_4{\cdot}yH_2O$ for all the exchanged products (Table 1).

As in normal ion exchange reactions, we expected that the ethylenediammonium cations would be replaced by an equivalent amount of metal ions. However, our observations suggest that in addition to the organic cations diffusing out of the structure, the phosphate groups linking VPO layers also leached out as a result of excess alkali metal cations [Equation (1)]. It seems that the amount of metal cations incorporated between the layers of the final products is essentially dictated by the charge present on the layers (equivalent to the amount of V^{4+} present). Also, the amount of water molecules entering between the layers depends on the nature of the cation. During the exchange reaction, the oxidation state of vanadium remained the same, i.e. no redox reaction occurred between the species present in the aqueous solution and the mixed-valent vanadyl phosphate. Since the product (M_xVPO) shows a strong structural resemblance to the parent phase (enVPO) along the [101] direction, the reaction can be considered as *topotactic*.[28] The structural change taking part in the exchange reaction is shown in Scheme 1. During the exchange reaction, ethylenediammonium groups are exchanged by metal ions. In addition, the phosphate groups linking the layers are leached out due to the presence of excess metal cations. The scheme also shows the reduction in the basal axis during the transformation. The exchange reaction can be written as in Equation (1).

Our results indicate that exchange reactions take place only when diameter of the monovalent cation is in the range of 2.7−3.0 Å, i.e. similar to the kinetic diameter of the ethylenediammonium cation (2.8 Å). The reaction with thallium ions led to the formation of a yet uncharacterised solid, $Tl_{0.45}VOPO_4{\cdot}0.33H_2O$. The mild conditions that we employed here imply a broad scope for investigating exchange reactions of other organically intercalated solids and, in particular, metal phosphates in order to obtain new metastable phases.

We also examined whether the ion-exchange behaviour of M_xVPO prepared by the topotactic reaction is similar to that reported in the literature for related systems. For example, K_xVPO exhibits facile and complete ion exchange with ammonium ions. A similar observation has been reported by Zima et al.[29] where the ion exchange ceased after 14 days at $x = 0.15$. However, in our case a complete

Table 1. Compositional analysis of M_xVPO

M in $M_xVOPO_4{\cdot}yH_2O$	Amount of metal intercalated,[a] x	No. of water molecules, y	Basal spacing [Å]	Ionic radius [Å][b]	Curie constant, C [emu K/mol]
K^+	0.53	1.15	6.33	1.38	0.38
Rb^+	0.57	1.22	6.40	1.52	0.39
Tl^+	0.54	0.33	6.54	1.50	0.41
$(NH_4)^+$	0.56	1.42	6.67	1.46	0.35
enVPO	–	–	7.89	–	0.40

[a] The value of x is equivalent to the amount of V^{4+} estimated from a cerimetric titration. [b] R. D. Shannon, *Acta Crystallog., Sect. A* **1976**, *32*, 751; radii based on coordination number 6.

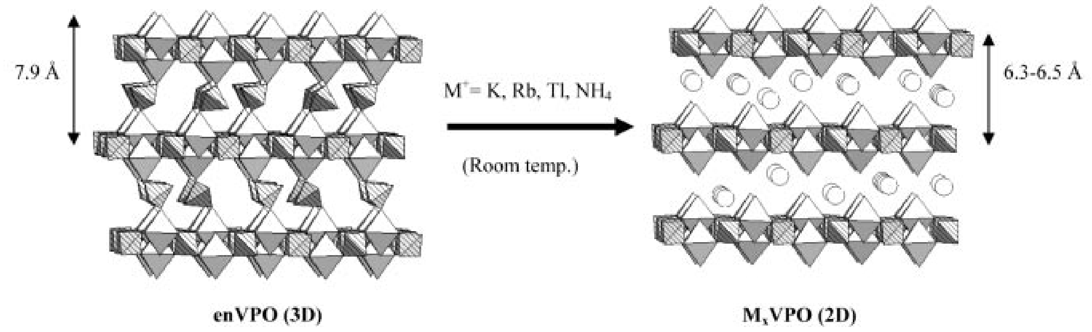

Scheme 1

conversion into $(NH_4)_xVPO$ was achieved within 2 days. The reverse reaction, i.e. conversion of $(NH_4)_xVPO$ to K_xVPO which has not reported so far, could also be achieved. However, in this case only partial ion exchange was observed (Figure 4). It is quite possible that the arrangement of the metal atoms and the stacking of vanadyl phosphate layers in M_xVPO may be different if the method of preparation is varied since a true equilibrium is possible only when crystals are grown under hydrothermal conditions. Powder X-ray diffraction is insufficient to give deeper insight into the complete crystal structure.

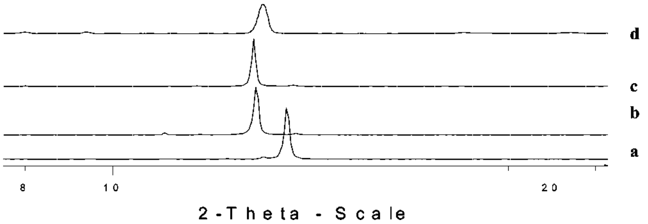

Figure 4. Powder X-ray diffraction patterns of (a) K_xVPO, (b) $(NH_4)_xVPO$ (c) ammonium exchanged K_xVPO and (d) potassium exchanged $(NH_4)_xVPO$

Magnetic Properties

Low-temperature magnetic measurements were performed on all metal exchanged products to establish the nature of their magnetic properties and spin concentrations. The magnetic behaviour of powdered samples of the mixed-valent M_xVPO is shown in Figure 5 in the form of a $1/\chi_m$ versus T plot. The susceptibility data for all samples were modelled over the temperature range 5 to 60 K according to the Curie−Weiss equation. While Rb_xVPO and K_xVPO showed ferromagnetic interactions, Tl_xVPO and $(NH_4)_xVPO$ showed antiferromagnetic interactions at low temperature. This behaviour is clear in the χ_mT versus T plots (Figure 6). The values of the Curie constants (0.38 and 0.39 emu K mol^{-1}) for the K and Rb compounds, respectively, are close to the values obtained for compounds of similar composition. Analogous behaviour was observed for the hydrothermally prepared $K_{0.5}VOPO_4{\cdot}2H_2O$ using the iodide method[30] and $NaBH_4$ as a reducing agent.[32] Our data is in accordance with that reported by Papoutsakis et al.[27] but is in contrast to the observations of Roca et al.[31] A plot of χ_mT versus T for $(NH_4)_xVPO$ and Tl_xVPO shows a strong deviation below 25 K indicating antiferromagnetic nearest-neighbour exchange interactions. Similar magnetic behaviour has been observed for $(NH_4)VOPO_4$ prepared under hydrothermal conditions.[33,34] A fully reduced thallium vanadyl phosphate $Tl_3(V^{IV}O)(HV_2{}^{IV}O_3)(PO_4)_2(HPO_4)$ and fully oxidised $Tl(V^VO_2)(HPO_4)$ were reported to be paramagnetic even at low temperatures.[35] However, mixed valent $Tl_6V_6P_6O_{31}$ showed low temperature antiferromagnetic behaviour.[36]

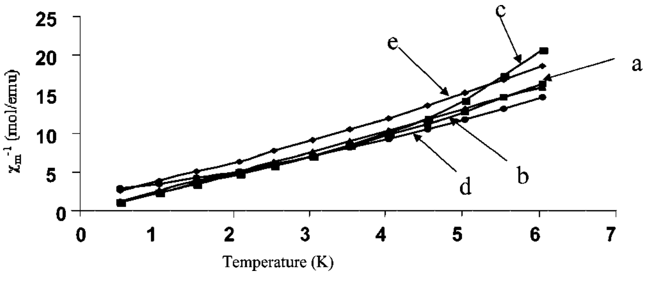

Figure 5. $\chi_m{}^{-1}$ versus temperature plots for (a) enVPO, (b) K_xVPO, (c) Rb_xVPO, (d) Tl_xVPO and (e) $(NH_4)_xVPO$; the susceptibilities have been corrected for the amount of reduced vanadium

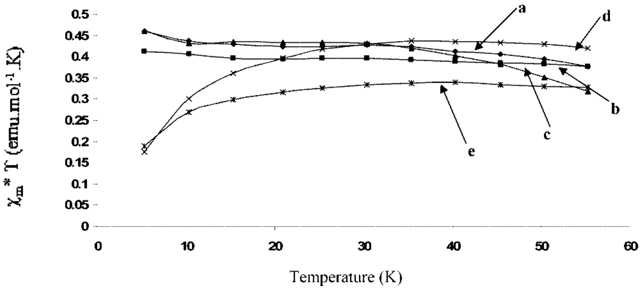

Figure 6. χ_mT versus temperature plots for (a) enVPO, (b) K_xVPO, (c) Rb_xVPO, (d) Tl_xVPO and (e) $(NH_4)_xVPO$; the susceptibilities have been corrected for the amount of reduced vanadium

Reactivity with Silver Ions

While the organic cation in enVPO could be readily exchanged with alkali metal or ammonium cations, different behaviour was observed with silver. A powder X-ray diffraction pattern of the product indicated a complete collapse of the parent layered structure. The reflections of this phase did not match with any of those reported previously. However, all peaks could be indexed to the monoclinic system with cell parameters, $a = 22.557(4)$, $b = 7.973(3)$ and $c = 12.430(3)$ Å and $\beta = 112.26(2)°$ using CRYSFIRE[37] (Figure 7).

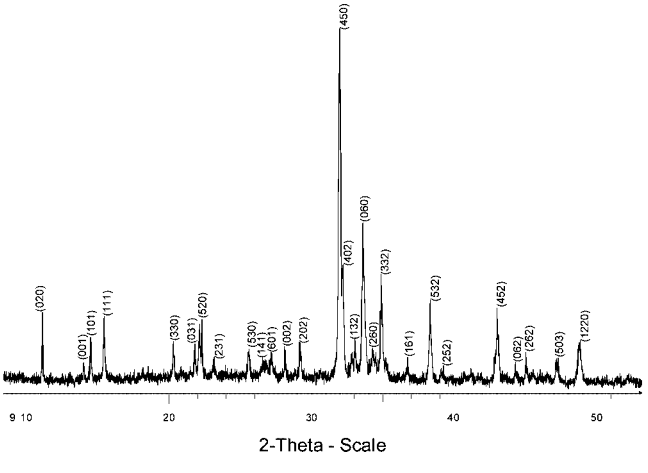

Figure 7. Powder X-ray diffraction pattern of $Ag_{3.5}VP_{1.5}O_8$

The solid did not show any appreciable weight loss as indicated by TG analysis (<3%) whereas DTA showed an endothermic peak around 620 K. TGA and DTA indicated the absence of organic groups which was further confirmed by FTIR spectroscopy and EDAX analysis. On the basis of

$$(H_3NCH_2CH_2NH_3)_{0.5}[V^{4+}{}_{0.45}V^{5+}{}_{0.55}O_2PO_4\{P(OH)_2\}_{0.483}] + 3.5Ag^+ \text{ (excess)} + H_2O \longrightarrow Ag_{3..5}VP_{1.483}O_{7..958} (\sim Ag_{3..5}VP_{1..5}O_8) + 2.966\ H^+ (aq) + 0.5\ (H_3NCH_2CH_2NH_3)^{2+} (aq) \qquad (2)$$

EDAX, we determined the approximate composition of the solid to be $Ag_{3.5}VP_{1.5}O_8$. Cerimetric titrations confirmed that the solid was a fully oxidised vanadium(v) phosphate. The reaction of silver ions with enVPO can be written as in Equation (2) and (3).

$$(H_3NCH_2CH_2NH_3)^{2+} \rightleftarrows (H_2NCH_2CH_2NH_2) + 2H^+ \longrightarrow Ag\text{ (metal)} \qquad (3)$$

To eliminate the possibility of photoreduction, the treatment of enVPO with silver ions was also carried out in dark. The products obtained under these conditions were identical. In order to confirm the presence of metallic silver and the cell parameters derived from powder X-ray pattern, we conducted electron microscopic studies on the silver exchanged enVPO product. The phase was found to be sensitive to the electron beam, resulting in rapid amorphisation. Transmission electron microscopic studies (Figure 8) clearly revealed the presence of nanospheres of silver metal particles (≈15 nm) decorated on plate like crystals of silver vanadyl phosphate. This was further confirmed by spot emission analysis. Since the fraction of silver metal in the sample was considerably low, its presence could not be observed in the powder X-ray diffraction pattern.

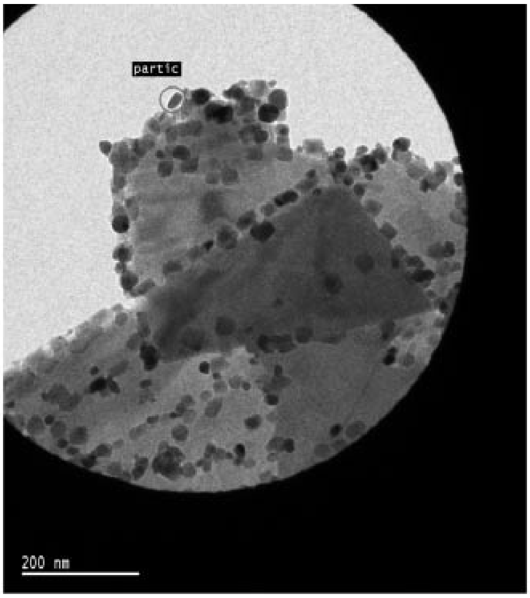

Figure 8. TEM of $Ag_{3.5}VP_{1.5}O_8$ showing nanoparticles of Ag (ca. 15 nm) on the AgVPO crystals

The exchanged products obtained in this work are all metastable. To probe the phase changes, if any, in $Ag_{3.5}VP_{1.5}O_8$, the sample was heated in air at various temperatures. A powder X-ray diffraction pattern showed (Figure 9) that the phase was stable up to 200 °C. Further heating in the temperature range 250 to 350 °C resulted in the loss of crystallinity. Interestingly, above 400 °C, $Ag_{3.5}VP_{1.5}O_8$ became completely transformed into a mixture of two thermodynamically stable phases, $Ag_2VO_2PO_4$ and Ag_3PO_4 [Equation (4)]. It should be remembered that TGA did not indicate any weight loss during this transformation. The presence of these two phases was further confirmed by refining the powder pattern using the Rietveld profile fitting technique (using TOPAS Version 2) on the basis of structural models reported for $Ag_2VO_2PO_4$ and Ag_3PO_4.[38,39] Using the software TOPAS 2, we also estimated the ratio of the two phases $Ag_2VO_2PO_4$ and Ag_3PO_4 to be 2:1 (Figure 10). On the basis of powder X-ray diffraction data and chemical analysis, we inferred the initial composition of the phase to be $Ag_{3.5}VP_{1.5}O_8$ according to the equation given below. EDAX analysis is also consistent with this observation.

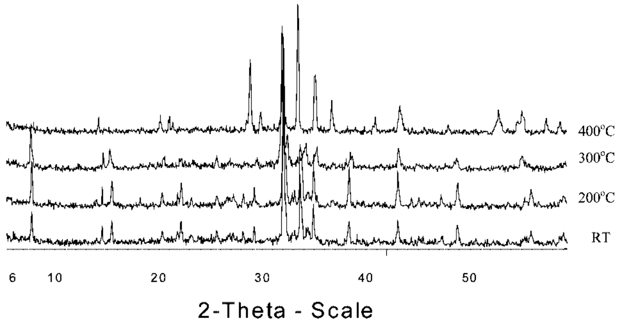

Figure 9. Powder X-ray diffraction patterns of $Ag_{3.5}VP_{1.5}O_8$ on heating: At 400 °C transformation to $Ag_2VO_2PO_4$ and Ag_3PO_4 takes place

$$Ag_{3.5}VP_{1.5}O_8 \xrightarrow{\Delta,\ 400^{\circ}C} Ag_2VO_2PO_4 + 0.5Ag_3PO_4 \qquad (4)$$

The structural change taking part in the exchange reaction with silver ions is shown in Scheme 2. During the exchange reaction, ethylenediammonium groups are exchanged by metal ions. Unlike alkali metal cations, the phosphate groups linking the vanadyl phosphate layers remain intact. It appears that the initial reaction of enVPO with silver ions occurs via ion exchange to form silver intercalated vanadyl phosphate. It appears that the weakly acidic ethylenediammonium cations appearing in the aqueous phase dissociate to form ethylenediamine which reduces silver ions to metallic silver [Scheme 2, Equations (2) and (3)]. This mechanism is quite probable in view of the electron microscopic observation that nanoparticles of silver metal are deposited on the edges of the plate-like crystals.

In order to rationalise the occurrence of excess silver in the phase, we further investigated room temperature reac-

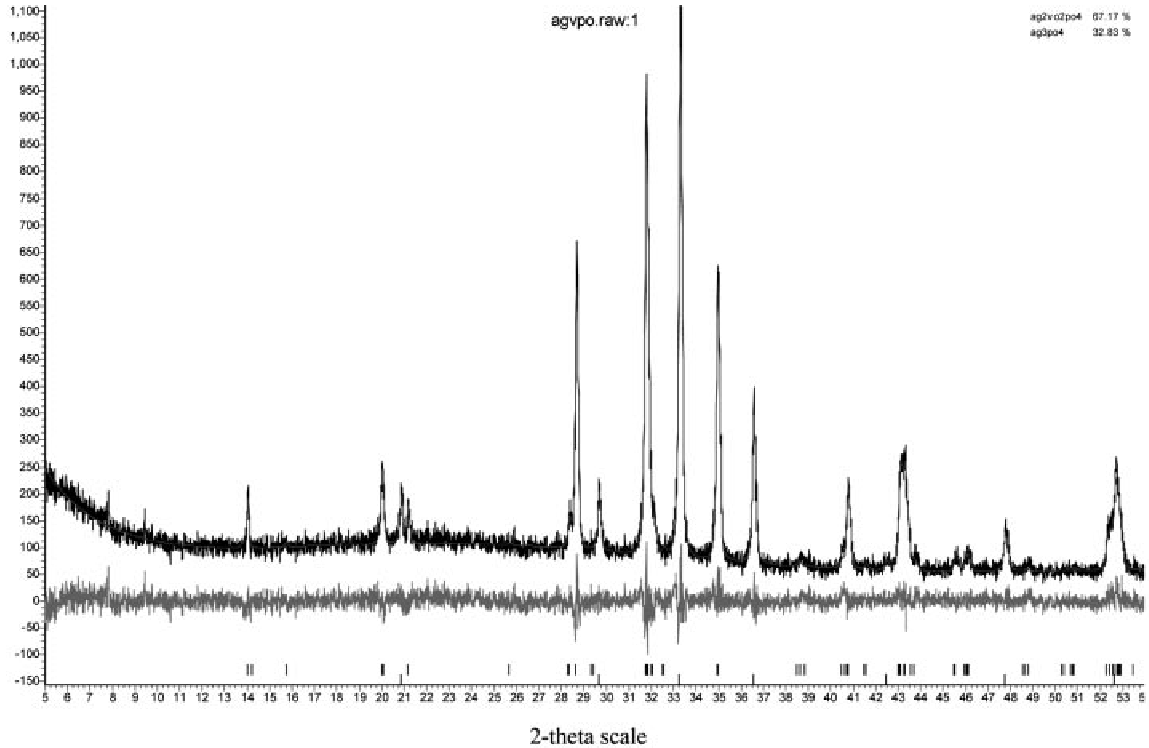

Figure 10. Quantitative phase analysis using TOPAS 2 of $Ag_{3.5}VP_{1.5}O_8$ heated at 400 °C

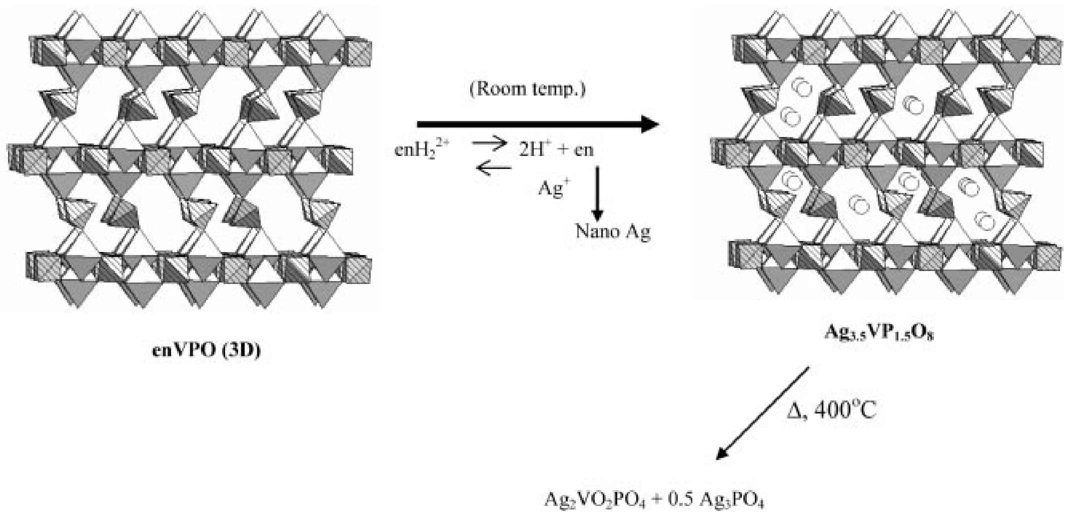

Scheme 2

tions of silver ions with other known vanadium phosphates such as $VOPO_4{\cdot}2H_2O$ and $VO(H_2PO_4)_2$. To our surprise, we obtained two possibly new phases whose powder X-ray patterns did not match with those of any other AgVPO phases reported in the literature. Also, the patterns did not show any resemblance to that of $Ag_{3.5}VP_{1.5}O_8$, suggesting that the reactions occur through different mechanisms. An EDAX analysis of the two phases indicated an Ag:V:P ratio of 2:1:1. SEM of the two solids revealed differences in morphology, i.e. a rod like morphology for the product from treatment of $VOPO_4{\cdot}2H_2O$ with silver whereas a globular morphology was observed for the phase resulting from treatment of $VO(H_2PO_4)_2$ with silver ions (Figure 11). The powder pattern of silver exchanged $VOPO_4{\cdot}2H_2O$ showed dominant 00l reflections and a basal spacing of 10.7 Å (Figure 12). However, all peaks corresponding to the solid obtained by treatment of $Ag^+(aq)$ with $VO(H_2PO_4)_2$ could be indexed to the monoclinic system with a = 10.904(7), b = 23.196(2), c = 5.680(2) Å and β = 96.83(4)° using CRYSFIRE[37] (Figure 13). Since single-crystals could not be grown for these metastable products, further structural characterisations of these new silver vanadium phosphates are currently being attempted using ab initio computer modelling methods. Interestingly, both products undergo

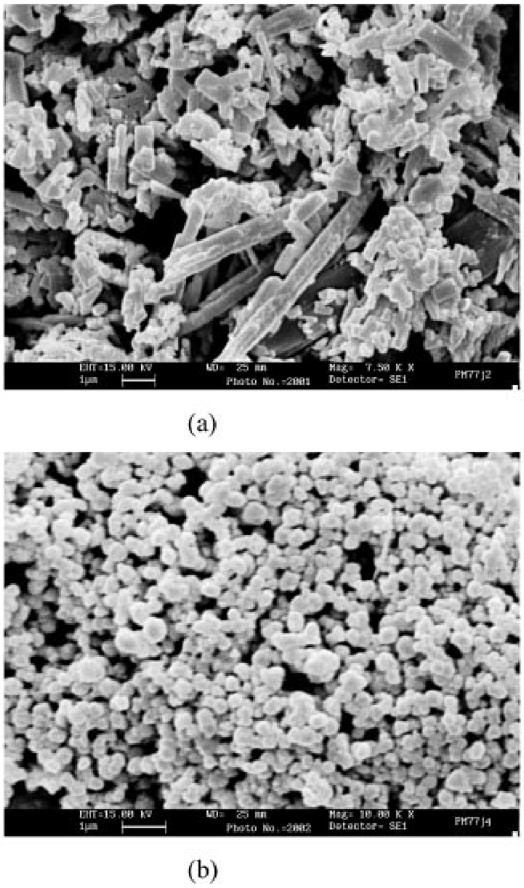

(a)

(b)

Figure 11. Scanning electron micrographs of silver exchanged (a) $VOPO_4 \cdot 2H_2O$ and (b) $VO(H_2PO_4)_2$

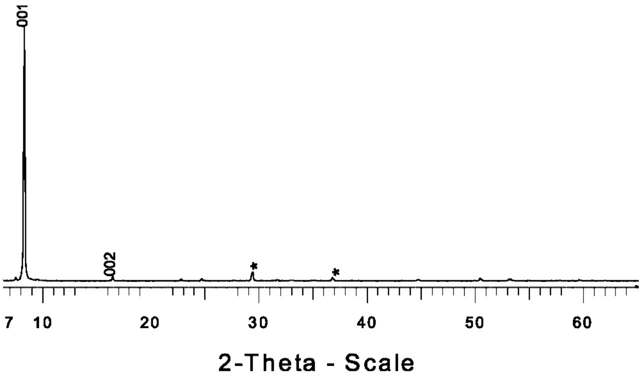

Figure 12. Powder X-ray diffraction pattern of the product obtained from the reaction of silver ions with $VOPO_4 \cdot 2H_2O$; * indicates reflections which have not been indexed

transformation to $Ag_2VO_2PO_4$ upon heating to around 100 °C in air confirming that the Ag:V:P ratio is 2:1:1. $Ag_2VO_2PO_4$ has also been prepared previously by a solid state reaction carried out at high temperatures (>500 °C).[38] However, our method appears to be a convenient low temperature route for the preparation of single phase $Ag_2VO_2PO_4$. It is significant to note that silver vanadium phosphates are mostly synthesised using solid-state reactions whereas the soft chemistry route remains somewhat unexplored. It appears from our work as well as from other reports available in the literature that vanadium based solids such as VO_2, V_2O_5, $NaVO_3$ etc. as well as vanadyl phosphates show unusual reactivity towards silver ions in aqueous solution at room temperature yielding fully oxidised vanadate or vanadium phosphate phases. For example, Kittaka[40] and Znaidi et al.[41] observed the formation of $AgVO_3$ by treatment of vanadium oxide xerogel with aqueous silver ions. We have also synthesised β-$AgVO_3$ nanorods coated with nanosilver through a reaction between organically intercalated vanadium oxides, $(org)_xV_2O_5$, with an excess of silver ions.[42,43] In this context, our observations and the earlier findings are quite significant for further investigations of the unusual reaction between vanadium compounds and silver ions. Further experiments are necessary to fully understand the reaction mechanism.

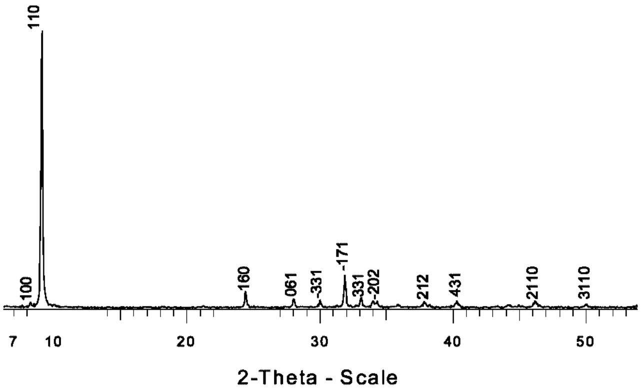

Figure 13. Powder X-ray diffraction pattern of the product obtained from the reaction of silver ions with $VO(H_2PO_4)_2$

Conclusions

The reaction of enVPO with suitably sized aqueous cations viz. K, Rb, Tl, NH_4 at room temperature is *topotactic* and forms intercalated vanadyl phosphates, $M_{0.45}VOPO_4 \cdot yH_2O$. Vanadyl phosphate shows unusual room temperature reactivity with silver ions under aqueous conditions. The reaction of enVPO with silver ions occurs through a different mechanism and forms a new metastable phase, $Ag_{3.5}VP_{1.5}O_8$. The current approach may be quite significant for the exploitation of using other organically intercalated phosphates in the formation of new phases particularly with alkali metal ions.

Experimental Section

Syntheses: All the reagents were obtained from Aldrich and were used without further purification. Ethylenediammonium intercalated vanadyl phosphate, $(H_3NCH_2CH_2NH_3)_{0.5}[V^{4+}_{0.45}V^{5+}_{0.55}O_2PO_4\{P(OH)_2\}_{0.483}]$ (enVPO) was synthesised by a hydrothermal reaction of ethylenediamine (en), vanadium pentoxide and phosphoric acid at 180 °C for 10 h as described earlier.[19] In a typical synthesis, V_2O_5 (0.2 g) was treated with H_3PO_4 (2 mL, 85%), en (0.17 mL) and distilled water (30 mL) in the molar ratio

V_2O_5:H_3PO_4:en:H_2O = 1:32.4:2.4:1515. The mixture was transferred to a 45 mL Teflon lined Parr acid digestion reactor and the reaction vessel was heated at 180 °C for 10 h under autogenous pressure before cooling to room temperature at 10 °C/h. The resultant green coloured powder was washed with distilled water, acetone and allowed to dry in air. Whenever we employed nickel or cobalt powder, we obtained a phase close to enVPO but with varying degrees in the oxidation state of the vanadium. In this work, the initial precursor enVPO was prepared in the absence of metal powders. Cerimetric titrations showed that the average oxidation state of vanadium was around 4.55. On the basis of EDAX, CHN analysis and cerimetric titration, we arrived at the approximate composition for enVPO given above. Exchange reactions were carried out by suspending enVPO (0.5 g) in an aqueous solution of the appropriate metal chlorides (75 mL, 2 M; for silver, silver nitrate was used) for two days at room temperature. Complete exchange took a longer time with lower concentrations of the metal salt (e.g. 4 d with 1 M and 6 d with 0.5 M aqueous solutions). With alkali metals and ammonium salts, there was no visible colour change. However, in case of silver ions, the progress of exchange was clearly evident from the colour change (from green to yellow) during the course of reaction. All the exchanged products were filtered, washed with distilled water and dried in air. A suspension of enVPO showed no reactivity towards lithium, sodium or divalent ions as shown by powder XRD, cerimetric titration, EDAX analysis and FTIR spectroscopy. For further ion exchanges of the layered VPO species synthesised in this study, M_xVPO (0.2 g) was suspended in an appropriate metal solution (0.5 g in 30 mL of distilled water) and stirred at room temperature (30 °C) for 2 d. The product was isolated by filtration, washed with distilled water and dried in air.

Methods: FTIR spectra were recorded in KBr pellets using a Nicolet 5DX spectrophotometer. TG/DT analyses were carried out using a Perkin−Elmer TGA7 and DTA7 system on well ground samples under a flow of nitrogen with a heating rate of 10 °C/min. SEM and EDAX were recorded using a Philips XL30 microscope. Room-temperature X-ray powder diffraction data were collected on a Bruker D8 Advance diffractometer using Ni-filtered CuK_α radiation. Data were collected with a step size of 0.02° and a count time of 2 s per step over the range $4° < 2\theta < 60°$. Transmission electron microscopic studies were carried out on a Philips CM 20 instrument operating at 200 kV. The susceptibility measurements as a function of temperature were performed with a SQUID magnetometer. Diamagnetic corrections were estimated using Pascal's constants. The average oxidation state of vanadium and the total vanadium content were determined using a cerimetric titration.

Acknowledgments

M. A. acknowledges CSIR for a fellowship. A. R. acknowledges DST under IRHPA for the powder X-ray diffraction facility to Department of Chemistry, IIT, Delhi. A. R. thanks Unispec Marketing, New Delhi, India, for providing the software, TOPAS version 2. KVR and SEL acknowledge the support of the New Jersey Commission on Higher Education through the High Tech Work Force Grant.

[1] G. Centi, F. Trifiro, J. R. Ebner, V. M. Franchetti, *Chem. Rev.* **1998**, *88*, 55−80.
[2] K. Beneke, G. Lagaly, *Inorg. Chem.* **1983**, *22*, 1503−1507.
[3] J. W. Johnson, A. J. Jacobson, J. F. Brody, S. M. Rich, *Inorg. Chem.* **1982**, *21*, 3820−3825.
[4] L. Benes, K. Melanova, V. Zima, J. Kalousova, J. Votinsky, *Inorg. Chem.* **1997**, *36*, 2850−2853.
[5] L. Benes, J. Votinsky, J. Kalousova, K. Handlir, *Inorg. Chim. Acta* **1990**, *176*, 255−259.
[6] M. Martinez-Lara, L. Moreno-Real, A. Jimenez-Lopez, S. Bruque-Gamez, A. Rodriguez-Garcia, *Mat. Res. Bull.* **1986**, *21*, 13−23.
[7] C. Costentin, L. Savary, J. C. Lavelly, M. M. Borel, A. Grandin, *Chem. Mater.* **1998**, *10*, 59−64.
[8] D. Beltran-Porter, A. Beltran-Porter, P. Amoros, R. Ibanez, E. Martinez, A. Le Bail, G. Ferey, G. Villeneuve, *Eur. J. Solid State Inorg. Chem.* **1991**, *28*, 131−161.
[9] S. Boudin, A. Guesdon, A. Leclaire, M. M. Borel, *Int. J. Inorg. Mater.* **2000**, *2*, 561−579.
[10] K. K. Rangan, J. Gopalakrishnan, *J. Solid State Chem.* **1994**, *109*, 116−121.
[11] P. Ayyappan, A. Ramanan, P. A. Joy, A. Pring, *Solid State Ionics* **1998**, *107*, 53−57.
[12] P. Ayyappan, A. Ramanan, C. Torardi, *Inorg. Chem.* **1998**, *37*, 3628−3634.
[13] K. H. Lii, H. J. Tsai, *Inorg. Chem.* **1991**, *30*, 446−448.
[14] L. Benhamada, A. Grandin, M. M. Borel, A. Leclaire, M. Leblanc, B. Raveau, *J. Solid State Chem.* **1992**, *96*, 390−396.
[15] M. L. F. Phillips, W.T.A. Harrisson, T. E. Gier, G. D. Stucky, G. V. Kulkarni, J. K. Burdett, *Inorg. Chem.* **1990**, *29*, 2158−2163.
[16] R. C. Haushalter, Z. Wang, M. E. Thompson, J. Zubieta, *Inorg. Chem.* **1993**, *32*, 3700−3704.
[17] L. F. Nazar, B. E. Koene, J. F. Britten, *Chem. Mater.* **1996**, *8*, 327−329.
[18] Y.-J. Liu, J. A. Cowen, T. A. Kaplan, D. C. DeGroot, J. Schindler, C. R. Kannewurf, M. G. Kanatzidis, *Chem. Mater.* **1995**, *7*, 1616−1624.
[19] P. Ayyappan, M. Asnani, A. Ramanan, Y. Piffard, *Proc. Ind. Acad. Sci. (Chem. Sci.)* **2003**, *115*, 33−40.
[20] W. T. A. Harrison, K. Hsu, A. J. Jacobson, *Chem. Mater.* **1995**, *7*, 2004−2006.
[21] V. Zima, L. Benes, K. Melanova, M. Vlcek, *J. Solid State Chem.* **2002**, *163*, 281−285.
[22] A. J. Jacobson, J. W. Johnson, J. F. Brody, J. C. Scanlon, J. T. Lewandowski, *Inorg. Chem.* **1985**, *24*, 1782−1787.
[23] V. Zima, L. Benes, J. Votinsky, J. Kalousova, *Solid State Ionics* **1995**, *82*, 33−38.
[24] A. Chauvel, M. E. de Roy, J. P. Besse, A. Benarbia, A. Legrouri, A. Barroug, *Mater. Chem. Phys.* **1995**, *40*, 207−211.
[25] V. Zima, M. Kilian, M. Casciola, L. Massinelli, *Chem. Mater.* **1999**, *11*, 3258−3262.
[26] J. W. Johnson, A. J. Jacobson, *Angew. Chem. Int. Ed. Engl.* **1983**, *22*, 412−413.
[27] J. Do, R. P. Bontchev, A. J. Jacobson, *Inorg. Chem.* **2000**, *39*, 3230−3237.
[28] J. W. Johnson, D. C. Johnston, A. J. Jacobson, J. F. Brody, *J. Am. Chem. Soc.* **1984**, *106*, 8123−8128.
[29] V. Zima, L. Benes, K. Melanova, J. Svoboda, *J. Solid State Chem.* **2004**, *177*, 1173−1178.
[30] D. Papoutsakis, J. E. Jackson, D. G. Nocera, *Inorg. Chem.* **1996**, *35*, 800−801.
[31] M. Roca, P. Amoros, J. Cano, M. D. Marcos, J. Alamo, A. Beltran-Porter, D. Beltran-Porter, *Inorg. Chem.* **1998**, *37*, 3167−3174.
[32] P. Ayyappan, PhD Thesis, Indian Institute of Technology, Delhi, **1999**.
[33] C. J. O′Connor, V. Soghomonian, R. C. Haushalter, Z. Wang, J. Zubieta, *J. Appl. Phys.* **1994**, *75*, 5859−5861.
[34] R. C. Haushalter, Q. Chen, V. Soghomonian, J. Zubieta, C. J. O′Connor, *J. Solid State Chem.* **1994**, *108*, 128−133.
[35] G. Huan, J. W. Johnson, A. J. Jacobson, E. W. Corcoran, D. P. Goshorn, *J. Solid State Chem.* **1991**, *93*, 514−525.
[36] B. B. Das, I. L. Benhamada, A. Grandin, M. M. Borel, A. Leclaire, B. Raveau, *Mater. Chem. Phys.* **1995**, *39*, 239−242.
[37] Robin Shirley, *CRYSFIRE V3.1*, **2000**.

[38] H. Y. Kang, S. L. Wang, P. P. Tsai, K. H. Lii, *J. Chem. Soc., Dalton Trans.* **1993**, 1525−1528.
[39] H. N. Ng, C. Calvo, R. Faggiani, *Acta Crystallogr., Sect. B* **1978**, *34*, 898−899.
[40] S. Kittaka, K. Matsuno, H. Akashi, *J. Solid State Chem.* **1999**, *142*, 360−367.
[41] L. Znaidi, N. Baffier, M. Huber, *Mater. Res. Bull.* **1989**, *24*, 1501−1514.
[42] S. Sharma, M. Jansen, A. Ramanan, *Solid State Ionics* **2004**, *170*, 93−98.
[43] S. Sharma, A. Ramanan, M. Panthöfer, M. Jansen, *Mater. Chem. Phys.*, paper accepted for publication.

Received June 5, 2004
Early View Article
Published Online November 24, 2004